Losses in electrostatic actuation: a key challenge for electrocaloric cooling devices

Elie ZOGHBI, Morgan ALMANZA, Martino LOBUE
Université Paris-Saclay, École Normale Supérieure Paris-Saclay, CNRS, Laboratoire SATIE, 91190 Gif-sur-Yvette, France

ABSTRACT – Cooling plays a vital role in daily life, accounting for around 10% of global electricity consumption [1]. Electrocaloric cooling is an emerging technology that offers a promising, energy-efficient alternative to traditional vapor compression technologies. The electrocaloric (EC) effect is a reversible temperature change triggered by the application or removal of an electric field. To achieve cooling, the EC material is alternately brought into contact with the hot and cold sides using electrostatic actuation (EA). However, EA currently entails significant losses caused by various interfacial and electrostatic effects. To study these detrimental effects, an experimental setup was built to characterize the electro-adhesion pressure (EAP) between the two films mimicking the EC device, with a focus on identifying the contribution of each loss component. Losses are characterized by comparing the maximum EAP before contact (actual force of EA) to the maximum post-contact EAP (losses of EA) under a DC voltage. Prior to this analysis, the triboelectric for PVDF was examined, and it was found to be a negligible contributor to losses. Results show that PVDF exhibits significantly higher losses than polypropylene (PP), while the similar pre-contact air gaps estimated for both materials confirm the theoretical model and validate the measurements. The contact adhesion forces have also been estimated, and unexpectedly, they are found to increase with applied voltage, confirming them as the primary loss mechanism in EA. This voltage-dependent behavior is attributed mainly to charge injection or diffusion bonding forces.

Keywords—Electrocaloric effect; Electrostatic actuation; Electro-adhesion pressure; Films

1. INTRODUCTION

The electrocaloric (EC) effect is a reversible temperature change that occurs when an electric field is applied or removed. Cooling devices harnessing the EC effect have been developed with potential applications in areas such as power electronics and personal thermal management [2], [3]. Electrostatic actuation (EA) is one of the most studied thermal management approaches for EC cooling and is the central focus of this article. The working principle of the EA is based on Coulomb's law: applying a voltage across two electrodes with a dielectric between them causes opposite charges to attract, pulling the movable plate toward the fixed one. In addition to EC cooling, EA is also widely used in microelectromechanical systems (MEMS), soft robotics, and haptic devices due to its precision, scalability, and fast response. The EC effect is used in the Brayton cooling cycle of the device discussed here (two isofield and two adiabatic processes). Both the EA process and the EC effect are schematized in Figure 1 as part of the cooling cycle [2].

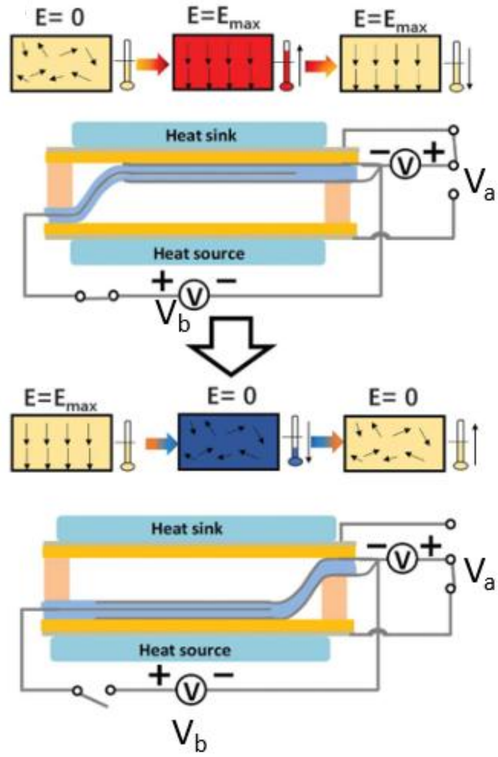

Figure 1. Cooling cycle with the EA process (V_a) and the EC effect (V_b), using trapezoidal voltages, during contact with the heat sink and heat source, respectively [2].

As shown in Figure 1, the device is composed of 3 films, from top to bottom: 1- An upper film (a yellow dielectric and a grey electrode) used for the EA; 2- A middle or EC film in S-shape (blue for the EC material and grey for its electrodes) to serve as a refrigerant; 3- A bottom film (a yellow dielectric and a grey electrode) used for the EA. There are 2 voltage sources: V_a for the EA and V_b for the EC effect. To drive the EC film upward, V_a is applied between the electrode of the upper film and the electrode of the middle film, and V_b is applied to get an electric field across the EC material so that it heats up, and the heat sink absorbs this heat by contact. Then, to move the refrigerant downward, V_a is applied between the electrode of the bottom film and the electrode of the middle film, and the applied voltage V_b is removed, allowing the EC material to cool and absorb heat from the heat source through direct contact. All the films have an 8×1 cm^2 surface. An 11 µm-thick PVDF film has been used with 4 nm thick gold electrodes.

Now, for the EA to work, the pure electro-adhesion pressure (EAP) (defined as an electrically controlled electrostatic attraction between two objects) must overcome the contact adhesion forces (defined as the force that maintains two materials together) like Van der Waals or capillary forces. Indeed, in standard conditions at a relative humidity of 50% and with a device using a gap of 100 nm, the Van Der Waals and capillary forces [4] can produce pressures of 1 Pa and 10 kPa, respectively. These pressures are close to the one achievable for the pure EAP, as reported in [5], and represent a major challenge to EA-based working devices. More concretely, there is a risk that the films stick to each other if the EA is not stronger than the contact pressure due to adhesion, but even if it works, the additional losses of the contact adhesion pressure must be accounted for. Here we shall address EAP between two films as the general adhesion pressure/force relevant in the device functioning, taking into account also the contact adhesion forces. The latter, as we shall show, depends on the applied voltage.

Additionally, today it is difficult to use theoretical models to get a reliable estimation of the different adhesion forces acting within the actual device. This is why the experimental setup of section 2 is proposed to address these and the previously mentioned challenges. Moreover, to reduce the losses associated with the EA as much as possible, a detailed study of the way the EAP evolves all along the actuation cycle and of the related losses is needed.

The article is organized as follows: after the introduction, we describe the experimental setup and the dielectric materials used. Then we discuss the importance of these two setups (namely the triboelectric and EAP setup) for unraveling EA losses. After this section, we show the results obtained and we include the difference in the results for Polypropylene (PP) and PVDF. We then provide a verification of the results of the EAP setup obtained (with respect to the theoretical model) and discuss two types of contact adhesion forces as the likely primary loss mechanisms of EA. At the end of the article, we present a conclusion summarizing the results obtained.

2. Electro-adhesion pressure experimental setup

As shown in Figure 2 (top left), the setup consists of a linear actuator that moves while a DC voltage is applied to the two electrodes, and the force and air gap distance are measured by a force sensor and a laser position sensor.

The building process of this setup was complicated and required synchronization between the measurements taken and the motion of the linear actuator. Indeed, beyond the hardware connections, DAQ system, and software, the setup required the use of very delicate thin films and the design and fabrication of numerous mechanical components to put together the full setup. As seen on the right-hand side of Figure 2, all the main components are attached to a black optical rail. The force sensor is attached to the moving linear actuator, and the movable upper film is attached to the force sensor. The laser position sensor is placed below the force sensor and measures the movement of the upper film. The fixed film is parallel to the movable upper film and is mounted on a square connected to the optical rail. As the linear actuator moves, the movable and fixed films have a cross-contact of $12 \times 12\ \mathrm{mm}^2$. Indeed, to have that cross-contact, the movable film is vertical while the fixed film is horizontal. Between the electrodes of the two films, a voltage is applied, and the current is measured.

In the setup which mimics the motion of the EA we can identify three main operating phases (bottom left of Figure 2) with a plot of force and air gap against time (taken from [5]): the approach and downward phase where the upper film approaches the bottom film at a constant speed until it makes contacts, the stationary and contact phase where the two films remain in contact for a set time, and the detachment phase where the upper film is raised up to its original position at a constant speed.

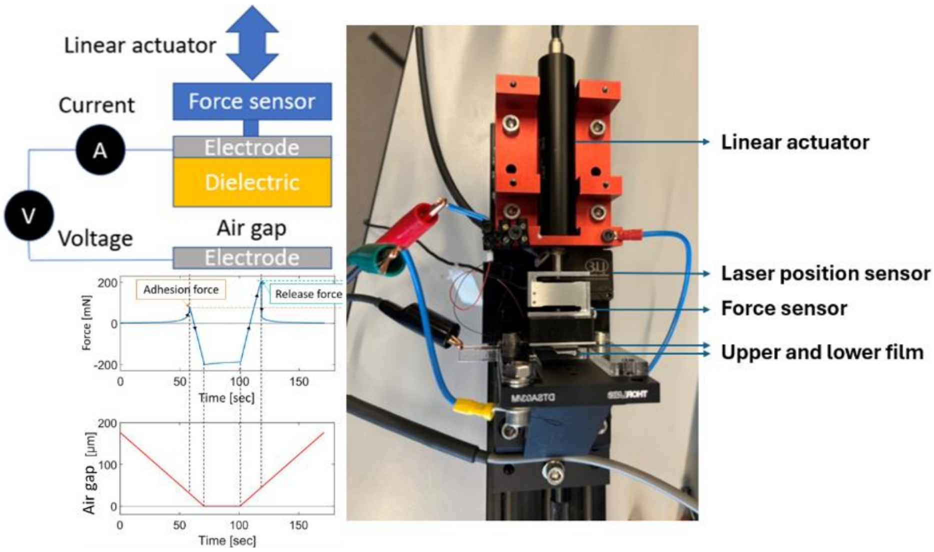

Figure 2. Setup used to measure the electro-adhesion pressure (EAP) and the triboelectric effect between the two films (top left of the figure). On the right-hand side, the main physical components of the setup are shown.

Only the middle and bottom films (yellow and grey layers of Figure 2) of the device shown in Figure 1 [2] are needed. This setup is devoted to the study of the pre-contact pressure, the contact pressure, and the post-contact detachment pressure with a focus on their maximum values. Similarly, using force and displacement sensors, the most significant results expected are plots as the ones shown in Figure 2 [5]. These plots will be analyzed during the three phases of the experiment. The analysis will involve comparing the maximum pressures recorded before and after contact. Additionally, it is crucial to examine the forces involved in the attachment and detachment processes. During attachment, the forces are typically weaker because of minimal or no surface interaction. In contrast, detachment forces are stronger, as they must overcome various interfacial forces. These contact adhesion forces include surface tension, Van der Waals forces, capillary forces, diffusion bonding forces, charge injection, and polarization effects [5].

2.1. *Goals of the setup*

The first goal is to measure the triboelectric effect with a surface contact between the two films (aluminum electrode with PVDF/PP dielectric) in which the linear actuator is used to separate and attach the two films while a current is measured between the two electrodes. This effect is a possible loss mechanism of the EA. In the triboelectric effect, the contact generates charges and voltage at the two terminals. It shows a strongly coupled effect between the mechanical and electrical parts of the system, which is why the experimental setup of this work, studying simultaneously the electric and the mechanical quantities, is original.

The second and more important goal is to measure the electro-adhesion force or EAP between the two films while the linear actuator moves (approach phase, stationary contact phase, and detachment phase), and a DC voltage is applied to the two electrodes (0 to 500 V). The force and air gap distance are measured by a force sensor and a laser position sensor. More in detail, the cross-contact area between the two films is 12×12 mm^2 (used to find the pressure from the force value), the film movement takes place over a 0.2 mm gap, a 300 mN contact force is applied during a 30 second holding time, and the speed of the moving film is 0.03 mm/s. This EAP experimental setup is similar to the one reported in [5] but with important differences (like the use of P(VDF-TrFE-CFE) instead of P(VDF-TrFE-C**T**FE)), and it is based on the device of Figure 1 [2].

2.2. Dielectric materials in the experimental setup

Now, regarding the materials used as a dielectric (yellow layer in Figure 2), one of the most promising candidates as an EC refrigerant is the P(VDF-TrFE-CFE) terpolymer (P, poly; VDF, vinylidene fluoride; TrFE, trifluoroethylene; CFE, chlorofluoroethylene) due to its large adiabatic temperature change. PVDF crystalline part can exist in different polymorphisms depending on the chain conformations, such as the paraelectric (PE) phase (i.e., alpha phase), the ferroelectric (FE) phase (i.e., beta phase), or (i.e., gamma phase) [6]. Although it is the material of interest for EC cooling, different phases of the PVDF introduce many additional effects, and therefore, to validate our result, we will use and start with a Polypropylene (PP) film as the well-known dielectric material. To summarize, we focus on the PVDF materials because of their high permittivity and the PP material serves as a reference due to its well-characterized dielectric properties. Moreover, PVDF is a ferroelectric material, and PP is a paraelectric material, meaning PP lacks complex polarization mechanisms. PP also allows the isolation of losses due to mechanical motion in the EA from those caused by other effects. Finally, these two materials allow us to distinguish between different adhesion mechanisms, particularly because PVDF is a polar material while PP is a non-polar material.

3. RELEVANCE AND RESULTS OF THE TWO SETUPS

3.1. Triboelectric setup

The reason we are interested in the triboelectric effect between the contact of the surfaces of the two films is that it is an energy dissipation mechanism or a loss and can prevent the EA from working. Indeed, at the contact, some of the motion or kinetic energy is converted to electrical energy, and the voltage generated by this effect can affect the existing charges of the EA. Compensating for this triboelectric effect by increasing the applied voltage may increase the post-contact EAP, resulting in an additional loss. In section 3.5, we shall show that this is because the contact adhesion forces increase with the voltage applied.

The idea of this test is to find the triboelectric charge density (TECD: σ_m) value (as documented in [7] for PP and PVDF) generated by the surface contact. The TECD value depends on the type of material and contact intimacy and is derived from the integral of the measured current. It is then used to estimate V_{tribo} as shown in equation (1) (d is the thickness of the dielectric: PVDF or PP). We can see that it is a loss of EA because as V_{tribo} increases the force of equation (2) decreases.

$$V_{tribo} = \frac{\sigma_m d}{\epsilon_0 \epsilon_r} \tag{1}$$

The estimate of the TECD value (results in Figure 3) was obtained by the process as part of the EAP setup built where the two films are in parallel, and motion is controlled by the linear actuator (process done without voltage (left plots) and with 300 V applied voltage (right plots) used only to have good contact between the two films). The setup presented here is more suitable for modeling the actual cooling devices, where thermal transfer is fostered by solid-solid contact, than the one presented in [7] based on solid-liquid contact.

3.2. Results of triboelectric setup

In terms of the result, the process yields small values of TECD and V_{tribo} or at least not as high as anticipated in the device. Therefore, contrary to expectations, the triboelectric effect is not the main cause of losses in the EA.

As shown in Figure 3, we can see both the current and the TECD values for the PVDF.

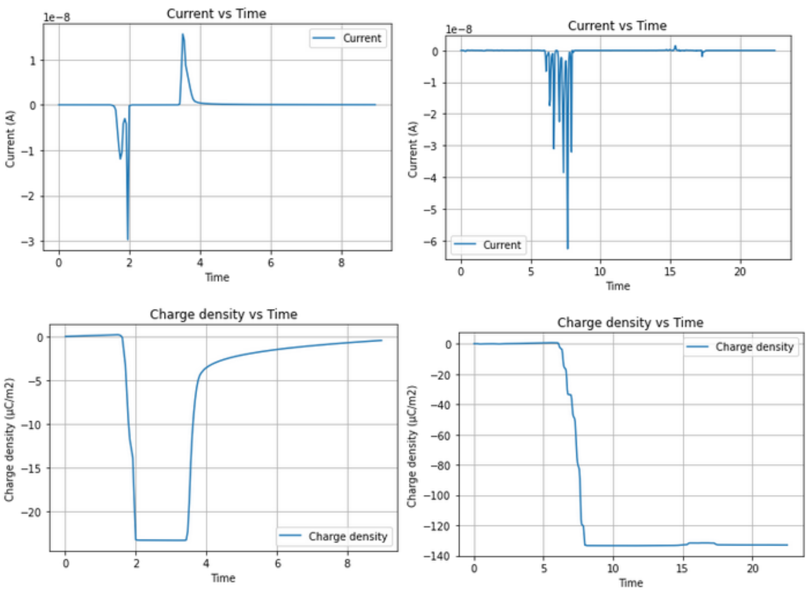

Figure 3. Plots of current and charge density (TECD) resulting from the triboelectric effect for PVDF. On the right, 300 V is applied to improve contact and the films are only separated.

For the plots on the left, at first there is contact between the two films, then a separation, and then an attachment between the two films (as in [7]) all during which is the current is measured. For the plots on the right, a voltage of 300 V is applied between the two films for better contact and is removed before separating them. The range of TECD values obtained for PVDF is between 25 and 132 $\mu C/m^2$ which yields a range of V_{tribo} between 0.43 and 2.3 V, negligible values as mentioned before. For information, PP has a TECD of 1.5 $\mu C/m^2$ and V_{tribo} values near 0.5 V.

3.3. EAP setup

To be clear, let us recall the definition of the electro-adhesion pressure called EAP. We consider it to be the general electrical adhesion pressure or force between two films, including not only electrostatic contributions but also all contact adhesion forces. As mentioned earlier, the main issue here is to use the measured EAP, as a function of time during the actuation process, as a tool for studying two key features: the maximum pre-contact and post-contact EAPs.

The maximum pre-contact EAP value represents the pure electrostatic force between the two films. This force is described by the following equation (with $V_{tribo} = 0$): S is the surface area of contact, e the air gap, and d the thickness of the dielectric (PVDF or PP) in the film.

$$F_{elec}(e, V_{eff}) = -\frac{\epsilon_0 S}{2}\left(\frac{V_{eff}}{e + \frac{d}{\epsilon_r}}\right)^2 \qquad (2)$$

$$V_{eff} = V_{applied} - V_{tribo} \qquad (3)$$

Indeed, whether the film moves up or down, the pre-contact electro-adhesion pressure (EAP) is always purely electrostatic, as there are no remaining contact forces once the film has fully detached. Additionally, triboelectric charges (TECD) are absent, since the charges had sufficient time to dissipate during the 30-second resting period with the previous film. This is further supported by the fact that the force plots were repeated consecutively and showed the same profile each time. This EAP value can be seen as the attraction force (or pressure) between the two films (to reach contact with the upper or lower film) for a given applied voltage. Up to a threshold, the larger this value is, the better it is for the EA. Note that in the device with no holding time, this pre-contact force would include a triboelectric component V_{tribo} which should in theory be independent of the voltage applied.

The second focus is on the maximum post-contact EAP value, which has three components: a non-pure electrostatic force component with an additional triboelectric component V_{tribo} due to the presence of triboelectric charges, and a contact adhesion force component (like Van Der Waals forces). This EAP value can be seen as the losses in the EA and a potential sticking issue that might prevent our device from working properly or reduce its efficiency.

These two EAP values and especially the losses, depend on the dielectric material of the moving film we tested namely the PP and PVDF. It is expected that the chosen PVDF material exhibits much higher losses than PP which needs to be verified and quantified.

3.4. Results of EAP setup

Now, we want to analyze the results obtained for PVDF. In Figure 4, as expected, we identify two peaks: one just before contact and one just after contact. We zoom in on the pre- and post-contact profiles in Figure 5. A holding time of 30 seconds (at contact) is maintained between the two peaks to allow all components of the contact adhesion force, regardless of their characteristic time, to become apparent in the plot.

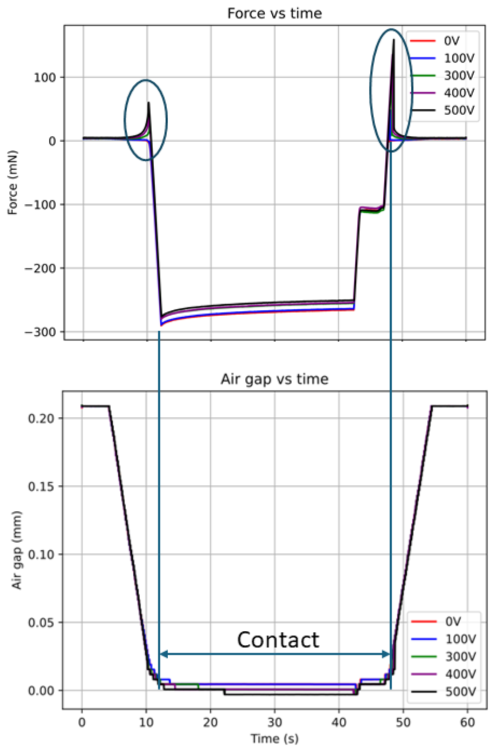

Figure 4. Plots of force and air gap versus time for PVDF. Each color corresponds to a different applied DC voltage: 0, 100, 300, 400, and 500 V.

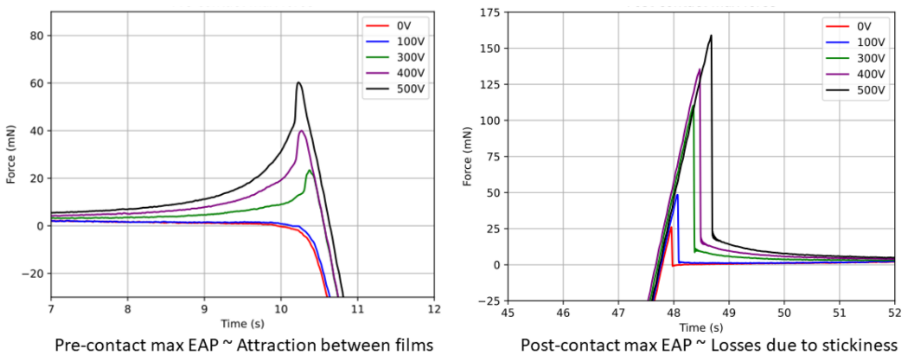

Figure 5. Zoomed-in view of the pre- and post-contact EAP profiles, as circled in Figure 4.

On the left side of Figure 5, we have the maximum pre-contact force value which corresponds to the attraction force between the two films. We can see that the force value is increasing and is an inverse-square function of the air gap distance ($F \propto \frac{1}{e^2(t)} \propto t^2$) as expected from equation (2). To obtain this, we assume that the air gap distance between the two plates is decreasing linearly over time ($e(t) \propto \frac{1}{t}$) and that $e(t) \gg \frac{d}{\epsilon_r} = \frac{11\ \mu m}{75}$. These assumptions are reasonable since the motion is done at a constant speed, and the air gap is very large before contact. On the right side of Figure 5, the profile represents the maximum post-contact force value which corresponds to the losses and adhesion forces between the two films after being in contact.

For the EA to work, these adhesion forces must be overcome by the attraction forces during the next EA cycle. However, in the actual device for the post-contact EAP we have that: 1- the voltage is removed before the end of the holding time, so the pure electrostatic component is removed, 2- there is a very small holding time, so the magnitude of the contact adhesion forces is much less but is still dominant with respect to the triboelectric component. Thus, in this EAP setup, the EA can work even if the value of the post-contact max EAP is larger than the value of the pre-contact max EAP.

As with the pre-contact peaks, the post-contact peaks also increase with voltage but show a stronger dependence on it. For example, the difference between the values at 100 V and 300 V is ~ 20 mN for the pre-contact peak and ~ 60 mN for the post-contact peak. To be rigorous on the force profile, we can see a small plateau close to $t = 45$ s which we confirmed via the air gap plot (not shown here) to be a vibration defect of our linear actuator and can be neglected as it should not have any effect on the post-contact maximum EAP value and profile.

3.5. *Comparison between PP and PVDF regarding the maximum EAP values*

The PP has a similar force profile (not shown here) with respect to the PVDF of Figure 4. In Figure 6, we can visualize the comparison between PP and PVDF.

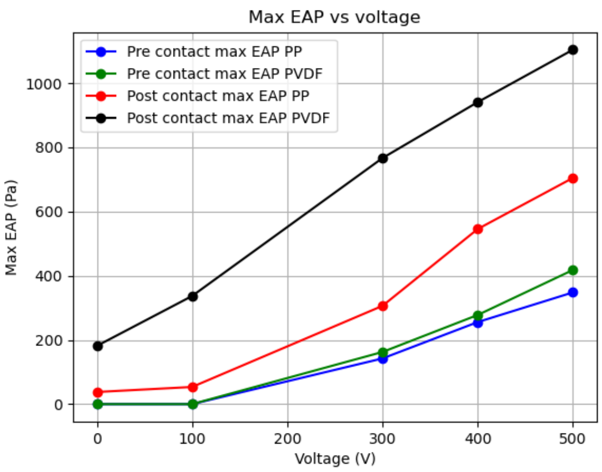

Figure 6. Plots of the maximum pre- and post-contact EAP values versus applied DC voltage for both PVDF and PP (0, 100, 300, 400, and 500 V).

In this Figure, the pre-contact max EAP values (green and blue curves) are similar for the two materials. This is expected from equation (2), in which only the thickness and the relative permittivity differ. However, there is a big difference between the post-contact max EAP values (black and red curves). This means that the PVDF material has much more losses than the PP in the device, seemingly because of higher contact adhesion forces and a higher triboelectric component.

We can now estimate the contact adhesion forces plus the triboelectric component, which is the difference between the post- and the pre-contact max EAP values at a given voltage. This is the case because they have a common component, namely the pure electrostatic force or pure EAP, which is subtracted. Contrary to what was expected, we notice that the contact adhesion forces are not constant and increase with the voltage applied, the triboelectric component being independent of voltage. For example, for PVDF, at 0, 100, 300, 400, and 500 V, the contact adhesion forces plus the triboelectric component have together a value of respectively 181, 337, 610, 663, and 686 Pa. For PP, for the same voltages, we have respective pressures of 38, 54, 164, 290, and 357 Pa. We notice that the contact adhesion forces are more sensitive to the increasing voltage values when the voltage is low for PVDF and when the voltage is high for PP.

The main finding here is that the increase in voltage increases the attraction between the films (same as pre-contact max EAP) and reduces the impact of the triboelectric component. At the same time, it increases the post-contact EAP values (because of contact adhesion forces), also known as the losses. Therefore, we need to find the best voltage of compromise to reduce the losses as much as possible. To be more concrete, we need to mainly change the maximum values of the trapezoidal voltages applied to the upper and lower film of the device, and possibly the period and rising time.

3.6. *Results verification of the EAP setup*

In the setup presented here (Figure 2), the estimate of the air gap is not very precise. Using the following equation

$$Air\ gap = V_{eff} \times \sqrt{\frac{\epsilon_0}{2EAP_{elec}}} - \frac{d}{\epsilon_r} \qquad (4)$$

based on equation (2)) and from the measured pre-contact EAP values (and corresponding voltage applied V_{eff} with $V_{tribo} = 0$), we can deduce its value for both PP and PVDF.

The pre-contact air gap estimated is near 50 µm and is the same for both PP and PVDF and for each different applied voltage V_{eff}. It is obtained with different pre-contact max EAP values. Therefore, this confirms the validity of the theoretical model with observations which imply that all the measurements taken are correct and performed under good conditions. It also means that the comparison done for PP and PVDF of section 3.5 is valid since the only difference for the pre- and post-contact EAP values is the dielectric material and the same contact force of 300 mN is chosen for all voltages.

It is also important to mention that the force or EAP profile obtained for P(VDF-TrFE-CFE) has a similar shape (for contact, pre-contact, and post-contact) as the profile obtained in [5] in Figure 2 for P(VDF-TrFE-CTFE) confirming the validity of the results obtained with materials chemically close to each other.

To confirm that the contact adhesion forces increase with the voltage applied, and to better model the actual EA in the device, the same EAP setup was used, but removing the voltage before the end of the 30 seconds holding time. Indeed, in this case, the post-contact max EAP value contains only a contact adhesion force and a triboelectric component, and no pure electrostatic component. The results obtained are in agreement with those of section 3.5 regarding the contact adhesion force sensitivity to voltage increase. More importantly, the results show that the contact adhesion forces increase with voltage but much more in the case of PVDF than PP, a difference more significant than what was obtained in section 3.5.

3.7. Contact adhesion forces as a source of EA losses

The observed increase in post-contact adhesion force with applied voltage (section 3.5) suggests a voltage-dependent mechanism, which cannot be explained by classical contact adhesion forces. Van der Waals interactions, surface tension, capillary forces, mechanical interlocking, and chemical bonding are either molecular in nature or depend on surface properties and environmental conditions, not on applied voltage or electric field strength [8].

Charge injection is the main mechanism that can produce strong, persistent adhesion that scales directly with voltage [5]. However, the effect of charge injection on adhesion between two dielectric films is complex and context-dependent. While some studies suggest that charge injections can increase adhesion due to trapped charges creating persistent electrostatic attraction [5], other studies have observed that excessive charge injections can lead to charge accumulation that may counteract adhesion forces, effectively reducing the overall contact adhesion force [9].

Therefore, we need an alternative and the most plausible explanation is the diffusion bonding contact adhesion force which depends on the intimacy of the contact which might increase with the increasing applied voltage, and it also depends on the duration of the contact (here 30 seconds). In addition, in polar polymers like PVDF, high electric fields may enhance interfacial diffusion through increased ionic or chain mobility or dielectric polarization [10]. However, a problem with that possibility is that in our results, we have nearly the same contact force and the same air gap of contact for all voltages, as can be seen in Figure 4.

In terms of the magnitude of the contact adhesion forces from section 3.5, at 0 V the Van der Waals forces are dominant since it is too weak (~ 181 Pa) to be due to diffusion bonding or other effects, and between 100 to 500 V, the force due to charge injection or the diffusion force is dominant. To conclude, it seems that either the diffusion bonding contact adhesion force or the contact adhesion force due to charge injection is the main loss mechanism of the EA and further analysis is required to distinguish between the two.

4. CONCLUSION

This work deals with the study of the losses in the electrostatic actuation (EA) of our electrocaloric (EC) cooling device, and using a specifically built setup for this purpose. The first result obtained indicates that for the P(VDF-TrFE-CFE) EC material, the triboelectric effect is not the main loss mechanism of the EA, with a low triboelectric charge density (TECD) value found. On the contrary, the contact adhesion forces, which surprisingly depend on the voltage applied between the two films, are found to be the main loss process in the EA for PVDF, especially compared to the PP material, which has much fewer losses. It seems that either the diffusion bonding contact adhesion force or the contact adhesion force due to charge injection is the primary component of this voltage-dependent contact adhesion force. This is deduced from the post-contact electro-adhesion pressure (EAP) maximum value, which represents the loss of the EA in the force profile. It is important to keep in mind that a decrease in the voltage applied between the two films reduces both the losses in the EA and its attraction force. Therefore, the voltage must be carefully optimized to achieve a compromise between minimizing losses and maintaining sufficient attraction force. Finally, to verify that all the tests and measurements were done under suitable conditions for both PVDF and PP, the pre-contact air gap values were estimated giving the same values for different applied voltages, and measured force values.

5. REFERENCES

[1] International Energy Agency, *The Future of Cooling: Opportunities for Energy-Efficient Air Conditioning*, Paris, France: IEA, 2018. [Online]. Available: https://www.iea.org/reports/the-future-of-cooling.

[2] R. Ma *et al.*, "Highly efficient electrocaloric cooling with electrostatic actuation," *Science*, vol. 357, no. 6356, pp. 1130–1134, Sep. 2017, doi: 10.1126/science.aan5980.

[3] Y. Meng *et al.*, "A cascade electrocaloric cooling device for large temperature lift," *Nat. Energy*, vol. 5, no. 12, pp. 996–1002, Oct. 2020, doi: 10.1038/s41560-020-00715-3.

[4] F. W. DelRio, M. P. De Boer, L. M. Phinney, C. J. Bourdon, and M. L. Dunn, "Van der Waals and Capillary Adhesion of Microelectromechanical Systems," in *Microelectromechanical Systems*, Chicago, Illinois, USA: ASMEDC, Jan. 2006, pp. 21–26. doi: 10.1115/IMECE2006-15169.

[5] S. Schaller and H. Shea, "Measuring electro-adhesion pressure before and after contact," *Sci. Rep.*, vol. 13, no. 1, p. 11768, Jul. 2023, doi: 10.1038/s41598-023-38872-6.

[6] N. Zeggai, M. Fricaudet, N. Guiblin, B. Dkhil, M. Lobue, and M. Almanza, "UV-A-Irradiated P(VDF-TrFE-CFE) as a High-Efficiency Refrigerant for Solid-State Cooling," *ACS Appl. Polym. Mater.*, vol. 6, no. 7, pp. 3637–3644, Apr. 2024, doi: 10.1021/acsapm.3c02562.

[7] H. Zou *et al.*, "Quantifying the triboelectric series," *Nat. Commun.*, vol. 10, no. 1, p. 1427, Mar. 2019, doi: 10.1038/s41467-019-09461-x.

[8] R. Maboudian and R. T. Howe, "Van der Waals and capillary adhesion of microelectromechanical systems," J. Vac. Sci. Technol. B, vol. 15, no. 1, pp. 1–20, Jan. 1997, doi: 10.1116/1.589207.

[9] Z. L. Wang and A. C. Wang, "On the origin of contact-electrification," Materials Today, vol. 30, pp. 34–51, May 2019, doi: 10.1016/j.mattod.2019.05.016.

[10] S. H. Tolbert et al., "Electric field induced phase transitions in polymers," Phys. Rev. Lett., vol. 108, no. 8, p. 087802, Feb. 2012, doi: 10.1103/PhysRevLett.108.087802.